



Comparison between M-score and LR-M in the reporting system of contrast-enhanced ultrasound LI-RADS

Li-Da Chen¹ · Si-Min Ruan¹ · Yuan Lin² · Jin-Yu Liang¹ · Shun-Li Shen³ · Hang-Tong Hu¹ · Yang Huang¹ · Wei Li¹ · Zhu Wang¹ · Xiao-Yan Xie¹ · Ming-De Lu^{1,3} · Ming Kuang^{1,3} · Wei Wang¹

Received: 9 May 2018 / Revised: 30 October 2018 / Accepted: 28 November 2018 / Published online: 19 December 2018
© European Society of Radiology 2018

Abstract

Objective To develop a contrast-enhanced ultrasound (CEUS) M-score and compare it with LR-M in CEUS Liver Imaging Reporting and Data System (LI-RADS).

Methods We retrospectively enrolled 105 consecutive high-risk patients with hepatocellular carcinoma (HCC) and 105 with intrahepatic cholangiocarcinoma (ICC). The subjects were selected by propensity score matching between November 2003 and December 2017. A CEUS M-score for predicting ICC was constructed based on specific CEUS features by the least absolute shrinkage and selection operator regularised regression. M-score was used to develop a modified CEUS LI-RADS. The diagnostic performance of the modified CEUS LI-RADS using M-score for diagnosing HCC and ICC was compared with American College of Radiology (ACR) CEUS LI-RADS using LR-M.

Results The most useful features for ICC were as follows: poorly circumscribed (69.52%), rim enhancement (63.81%), early washout (92.38%), intratumoural vein (56.19%), obscure boundary of intratumoural non-enhanced area (57.14%), and marked washout (59.05%, all $p < 0.001$). For predicting ICC, the M-score had a higher specificity (88.57% vs. 63.81%) with lower sensitivity (89.52% vs. 95.24%) compared with LR-M. For diagnosing HCC, the sensitivity of modified LI-RADS (80.95%) was much higher than that of ACR LI-RADS (57.14%), but the specificity was lower (90.48% vs. 96.19%). The area under the curve (AUC) of modified LI-RADS (0.857) was much higher than that of ACR LI-RADS (0.767, $p = 0.0001$). The modified positive predictive value (PPV) of ACR LI-RADS and modified LI-RADS were 99.42% and 98.99%, respectively.

Conclusions The modified LI-RADS with M-score had higher sensitivity for diagnosing HCC and higher specificity for diagnosing ICC than ACR LI-RADS.

Key Points

- For predicting ICC, the M-score had a higher specificity (88.57% vs. 63.81%) with lower sensitivity (89.52% vs. 95.24%) compared with LR-M.
- A CEUS M-score for predicting ICC consisted of more detailed CEUS features (poorly circumscribed, rim enhancement, early washout, intratumoural vein, obscure boundary of intratumoural non-enhanced area, and marked washout) was constructed.
- For diagnosing HCC, the sensitivity of modified LI-RADS (80.95%) was much higher than that of ACR LI-RADS (57.14%), but the specificity was lower (90.48% vs. 96.19%). The modified positive predictive value (PPV) of ACR LI-RADS and modified LI-RADS were 99.42% and 98.99%, respectively.

Keywords Ultrasonography · Hepatocellular carcinoma (HCC) · Hepatitis

Li-Da Chen and Si-Min Ruan contributed equally to this work.

✉ Wei Wang
wangw73@mail.sysu.edu.cn

¹ Department of Medical Ultrasonics, Institute of Diagnostic and Interventional Ultrasound, The First Affiliated Hospital of Sun Yat-Sen University, 58 Zhongshan Road 2, Guangzhou 510080, People's Republic of China

² Department of Pathology, The First Affiliated Hospital of Sun Yat-Sen University, Guangzhou, China

³ Department of Hepatobiliary Surgery, The First Affiliated Hospital of Sun Yat-Sen University, Guangzhou, China

Abbreviations

AASLD	American Association for the Study of Liver Diseases
ACR	American College of Radiology
AFP	Alpha-fetoprotein
AUC	Area under the curve
BUS	Baseline ultrasound
CEUS	Contrast-enhanced ultrasound
HCC	Hepatocellular carcinoma
ICC	Intrahepatic cholangiocarcinoma
LASSO	Least absolute shrinkage and selection operator
LI-RADS	Liver Imaging Reporting and Data System
NPV	Negative predictive value
PPV	Positive predictive value
ROC	Receiver operating characteristic

Introduction

The value of contrast-enhanced ultrasound (CEUS) for diagnosing hepatocellular carcinoma (HCC) in high-risk patients has been controversial in recent years [1–3]. In the 2005 edition of American Association for the Study of Liver Diseases (AASLD) guidelines of the management of HCC, CEUS was introduced as one of the dynamic diagnostic imaging modalities [4]. However, it was eliminated from the HCC diagnostic flowchart in the updated 2011 guidelines [5]. This deletion was mainly caused by a study [6] which concluded that intrahepatic cholangiocarcinoma (ICC) in cirrhosis shares a similar enhancement pattern to that of HCC on CEUS (47.6%, 10/21), which may lead to a false-positive diagnosis of HCC. This removal has caused a worldwide controversy and has not gained acceptance in some countries [3, 7–9] because the study was based on a small sample size without differential diagnostic analysis between ICC and HCC.

In 2016, the American College of Radiology (ACR) released the CEUS Liver Imaging Reporting and Data System (LI-RADS) [10]. It was designed in such a way that LR-5 could provide the highest specificity to diagnosing HCC and that HCC could be diagnosed by the criterion of LR-5 and send patients to treatment without biopsy. Terzi E et al found a high positive predictive value (PPV) of 98.5% in predicting HCC [11]. The CEUS LI-RADS also includes a category of lesions that are either definitely or probably malignant, named LR-M, which is not specific for HCC. This category may be the possibility of ICC, mixed hepatocellular and cholangiocellular carcinoma or other malignancies. In fact, there are studies which showed that 35–48% of LR-M lesions were HCCs, indicating a high false negative rate and low sensitivity for HCC diagnosis [11, 12]. In the CEUS LI-RADS algorithm, besides the major imaging features for diagnosis, ancillary features are also important to refine the final category [12]. Benefit to the real-time scanning of CEUS,

more dynamic and transient features would be explored to improve the system.

In light of the diagnostic issues of HCC and ICC, we sought to validate the diagnostic performance of HCC and ICC via the CEUS LI-RADS algorithm in our institute. Moreover, we identified important imaging predictors of ICC on CEUS, to develop an M-score that could be used to accurately predict the risk of ICC in high-risk patients and investigate the diagnostic performance of HCC and ICC with the modified CEUS LI-RADS.

Materials and methods

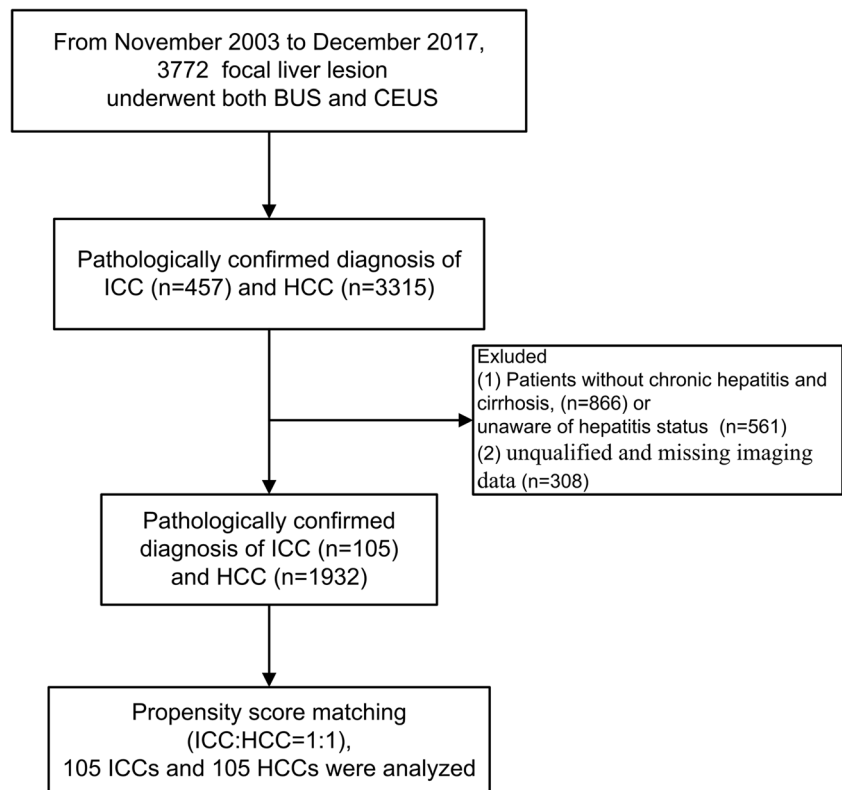
Patients

This study was approved by the institutional review board, and informed consent was obtained from each patient. From November 2003 to December 2017, 3315 consecutive patients with HCC and 457 consecutive patients with ICC who underwent both baseline US and CEUS were enrolled. The inclusion criteria were (1) a pathologically confirmed diagnosis of HCC or ICC and (2) high-risk patients with chronic hepatitis B infection confirmed via laboratory tests [13] and cirrhosis of any cause confirmed by pathological examination via liver biopsy or surgery. The exclusion criteria included (1) mixed hepatocellular cholangiocarcinoma ($n = 49$) or (2) unqualified and missing imaging data ($n = 308$).

Next, 1932 patients with HCC and 105 patients with ICC were included for propensity score matching, which was used to reduce the effect of selection bias in retrospective observational studies [14]. HCC and ICC patients were matched 1:1 using the nearest modality. The variables for matching were size and number of nodules. Finally, 105 patients with HCC and 105 patients with ICC were analysed in our study (Fig. 1). Basic clinical data including age and sex, as well as laboratory tests including hepatitis status, alpha-fetoprotein (AFP) levels, and CA-199 levels were recorded.

Image techniques

The ultrasound equipment was as follows: (1) Acuson Sequoia 512 with a 4 V1 vector transducer (frequency range, 1.0–4.0 MHz) and a contrast-specific mode of contrast pulse sequencing; (2) Aplio SSA-770 or Aplio 500 with a 375BT convex transducer (frequency range, 1.9–6.0 MHz) and a Contrast Harmonic Imaging mode; and (3) Aixplorer Ultrasound system equipped with the SC6–1 convex probe (frequency range, 1.0–6.0 MHz). All examinations were separately performed by two skilled radiologists (W.W. and X.Y.X.) who each had at least 15 years of experience in liver CEUS. First, the entire liver was scanned with baseline ultrasound (BUS). Then, the imaging mode was changed to CEUS,

Fig. 1 Diagram of the HCC and ICC patient selection

and a volume of 2.4 mL of SonoVue was administered. For patients with multiple nodules, only the largest lesion was selected. The target lesion was observed continuously for at least 3 min, and all imaging data were recorded. The CEUS process was classified into arterial (6–40 s after contrast agent injection), portal venous (41–120 s), and late phases (121–300 s).

All BUS and CEUS images were anonymised, randomised, and independently reviewed in two separate review sessions by two radiologists (L.D.C. and J.Y.L.), who had at least 10 years of experience in liver CEUS. Neither the patient details nor the clinical or pathological results were available to them. In cases of discordance, a third investigator (M.D.L., with at least 15 years of experience in liver CEUS) reviewed the images to make the final decision. The readers were simply asked to review the enhancement appearances of the lesion instead of making a diagnosis. Therefore, the readers were informed of the fact that all patients had either ICC or HCC, but they were blinded to the final diagnosis of the target lesion.

Image analysis

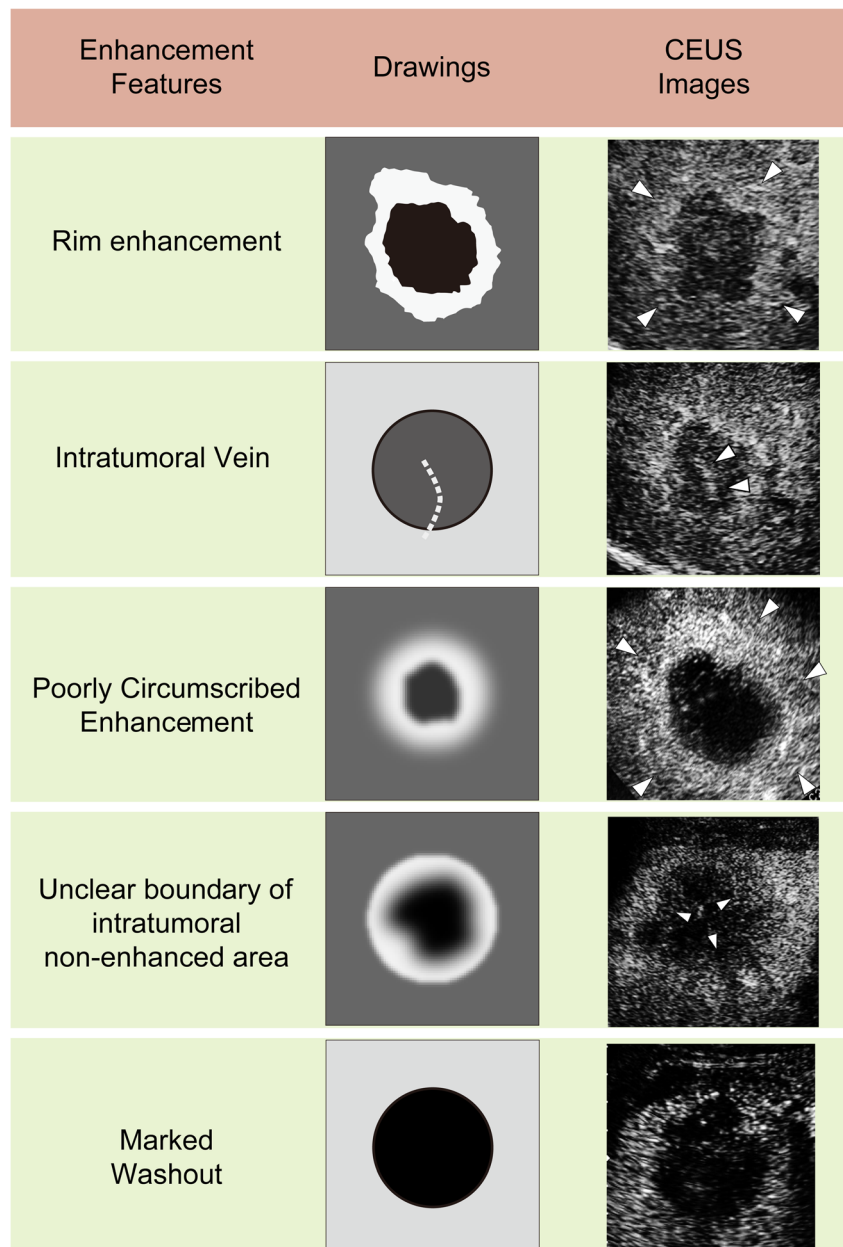
The CEUS features were characterised as follows (Fig. 2): (1) the number of lesions; (2) maximum diameter of the target nodule; (3) shape of the nodule; (4) boundary of the lesion; (5) enhancement level in the arterial/portal/late

phase (hyper-/iso-/hypo-); (6) enhancement patterns of the lesion in the arterial phase (rim/homogeneous/inhomogeneous/others); (7) time of enhance onset; (8) washout time (within 60 s or not) [15]; (9) duration of enhancement (washout time subtracts time of enhance onset, if the lesion showed hyperenhancement and then washout); (10) tumour supply artery (defined as an artery extending from the surrounding liver parenchyma into the tumour) [16]; (11) peripheral circular artery (defined as an annular strip artery around the tumour in the arterial phase) [16]; (12) intratumoural vein (defined as straight vessel branches extending through the mass during the portal venous and late phase) [17, 18]; (13) boundary of the intratumoural non-enhanced area (if it was present); and (14) marked washout (defined as the lesion appearing as a uniform black defect within the enhanced liver parenchyma) [15]. Histopathological examination was the reference standard of this study.

Development of M-score for predicting ICC

Because of the multicollinearity of the CEUS features, we used a method of least absolute shrinkage and selection operator (LASSO) [19] regularised regression to select the specific independent features for predicting ICC. A CEUS M-score for identifying ICC was developed via a linear

Fig. 2 Specific CEUS features of ICC



combination of selected features that were weighted by their respective coefficients.

Validation of modified CEUS LI-RADS with M-score

Using a modified CEUS LI-RADS diagnostic algorithm, that is, replacing the LR-M with the M-score, we then investigated the diagnostic performance of HCC and ICC. ICC was classified using the M-score. The cutoff value was determined by receiver operating characteristic (ROC) analysis. The remaining lesions were assigned to LR-3, LR-4, and LR-5 using the ACR CEUS LI-RADS Diagnostic Table. HCC was defined using the algorithm of LR-5 in ACR CEUS LI-RADS.

Validation of CEUS LI-RADS with LR-M

According to the CEUS LI-RADS, we classified the lesion as ICC using the definition of LR-M: rim enhancement in the arterial phase and/or early onset washout (< 60 s) and/or a marked (punched-out) appearance [20]. After the LR-M nodules were categorised, the rest of the lesions were assigned to LR-3, LR-4, and LR-5 categories referred to the CEUS LI-RADS Diagnostic Table. HCC was defined using the definition of LR-5: size ≥ 10 mm, typical arterial phase hyperenhancement (not rim or peripheral discontinuous globular), and late washout onset (≥ 60 s) with mild washout degree (15).

Statistical analysis

Statistical analysis was performed using R software (R Foundation for Statistical Computing, version 3.2.5, <http://www.r-project.org/>) and Medcalc (version 11.2). Significance was set at a two-tailed $p < 0.05$.

Categorical variables were compared with the χ^2 test. Continuous variables were compared with independent t test. The diagnostic performance of HCC and ICC was assessed by sensitivity, specificity, PPV, and negative predictive value (NPV). The area under the ROC curve (AUC) was calculated.

Results

Patients

One hundred and five ICC and 105 HCC nodules were observed. The study group comprised 210 nodules in 210 patients (72 men and 33 women; mean age \pm standard deviation, 54 years \pm 11 for the ICC group; 91 men and 14 women; mean age \pm standard deviation, 55 years \pm 10 for the HCC group) (Table 1). There were more male patients with HCC than with ICC ($p = 0.003$). Hepatitis B was confirmed in 101 (96.2%)

ICC patients, as well as in 103 (98.1%) HCC patients. Hepatitis B and C were confirmed in 4 (3.8%) ICC patients, as well as in 2 (1.9%) HCC patients. Alpha-fetoprotein (AFP) was elevated ($> 20 \mu\text{g/L}$) in 16 (15.2%) ICC patients and 49 (46.7%) HCC patients ($p < 0.0001$). CA19-9 was elevated ($> 35 \text{ U/mL}$) in 43 (41.0%) ICC patients and 10 (9.5%) HCC patients ($p < 0.001$). The number of nodules ≤ 3.0 cm, 3.1–5.0 cm, and > 5.0 cm was 10, 19, 76 in ICC group and 15, 28, 62 in HCC group, respectively ($p = 0.126$). There were 76 ICC patients (72.4%) and 82 HCC patients (78.1%) with one nodule, and 29 ICC patients (27.6%) and 23 HCC patients (21.9%) with multiple nodules ($p = 0.424$, Table 1).

Specific CEUS features of HCC or ICC

In HCC, the following features were observed more frequently than in ICC: hyperenhanced in arterial phase ($n = 102$, 97.14%), tumour supply artery ($n = 64$, 60.95%), and peripheral circular artery ($n = 29$, 27.62%) (all $p < 0.05$). On the other hand, the following features were observed more frequently in ICC than in HCC: poorly circumscribed ($n = 73$, 69.52%), iso- or hypo-enhanced in arterial phase ($n = 14$, 13.33%), hypoenhancement in the portal ($n = 103$, 98.10%), rim enhancement ($n = 67$, 63.81%), early washout ($n = 97$, 92.38%), short duration of enhancement ($n = 84$, 80.0%), intratumoural vein ($n = 59$, 56.19%), obscure boundary of intratumoural non-enhanced area ($n = 60$, 57.14%), and marked washout ($n = 62$, 59.05%) (all $p < 0.05$) (Fig. 3).

Table 1 Demography of patients with an HCC or ICC

Characteristic	ICC	HCC	<i>p</i>
Number of patients	105	105	
Gender			0.003
Male	72 (68.6)	91 (86.7)	
Female	33 (31.4)	14 (13.3)	
Age (years) ^a	54 \pm 11 (32–84)	55 \pm 10 (32–84)	0.564
Hepatitis status			0.679
Hepatitis B	101 (96.2)	103 (98.1)	
Hepatitis B + C	4 (3.8)	2 (1.9)	
AFP > 20 ($\mu\text{g/l}$)	16 (15.2)	49 (46.7)	< 0.001
Ca 19–9 > 35 (U/ml)	43 (41.0)	10 (9.5)	< 0.001
Nodule size			0.126
≤ 3.0 cm	10 (9.5)	15 (14.3)	
3.1–5.0 cm	19 (18.1)	28 (26.7)	
> 5.0 cm	76 (72.4)	62 (59.0)	
Number of nodules			0.424
One	76 (72.4)	82 (78.1)	
Multiple	29 (27.6)	23 (21.9)	

Unless otherwise indicated, data are number of nodules, with percentages in parentheses

^aData are means \pm standard deviations, with ranges in parentheses

M-scoring for predicting ICC

The most useful CEUS independent variables for predicting ICC selected by LASSO regression were as follows: poorly circumscribed, rim enhancement in the arterial phase, rapid washout (within 60 s), intratumoural vein, boundary of the intratumoural non-enhanced area, and marked washout. The M-score for diagnosing ICC was developed based on the above independent variables:

$$\text{M-score} = -1.876 + 0.716 \times \text{poorly circumscribed} + 1.222 \times \text{rim enhancement} + 1.017 \times \text{rapid washout} + 0.321 \times \text{intratumoural vein} + 0.707 \times \text{unclear boundary of the intratumoural non-enhanced area} + 1.039 \times \text{marked washout}.$$

For diagnosing ICC, the sensitivity, specificity, PPV, NPV, and accuracy using the M-score as criterion were 89.52%, 88.57%, 88.68%, 89.42%, and 89.05%, respectively. The sensitivity, specificity, PPV, NPV, and accuracy using LR-M as criterion were 95.24%, 63.81%, 72.46%, 93.06%, and 79.52%, respectively (Table 2).

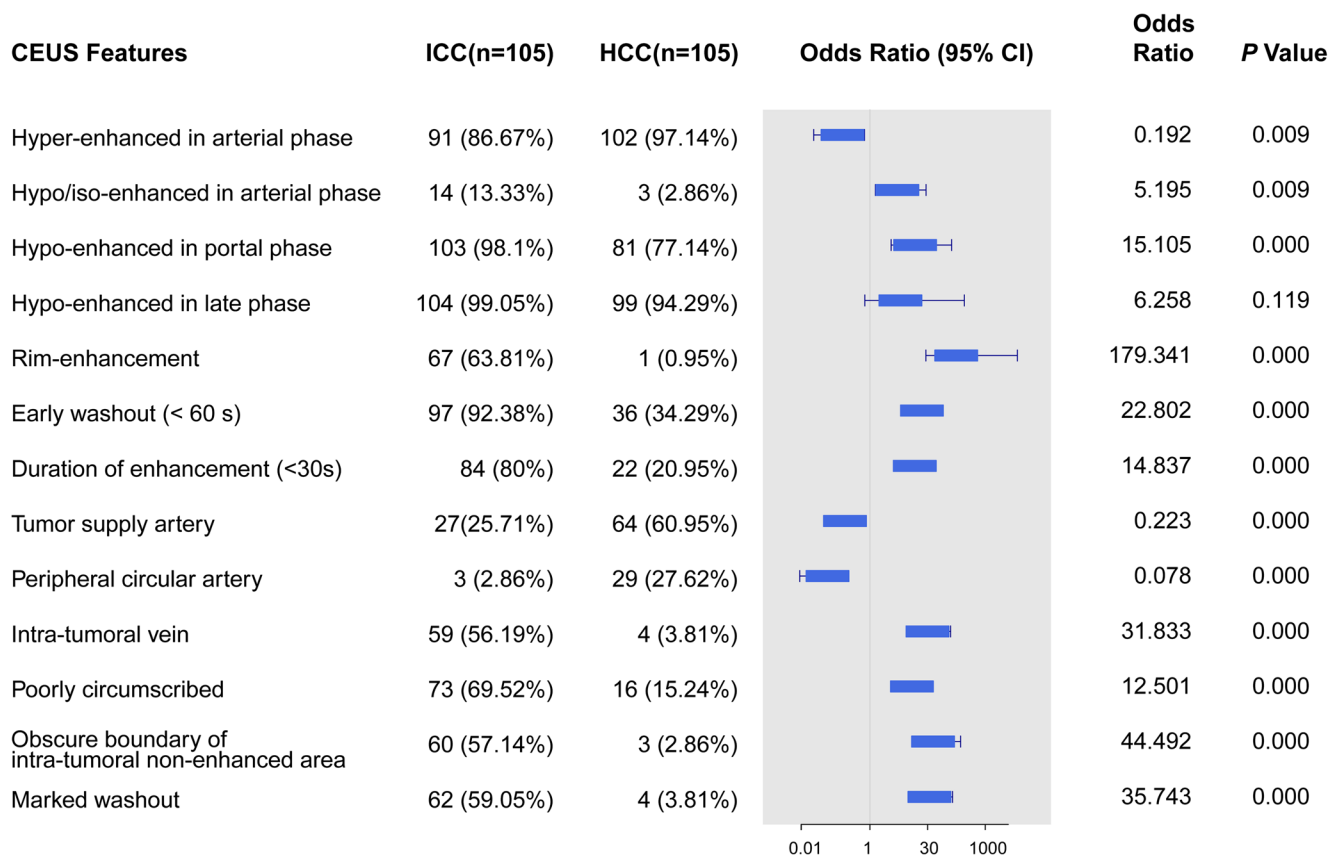


Fig. 3 Forest plot of CEUS features of HCC and ICC

Classification of HCC by ACR LI-RADS with LR-M or modified LI-RADS with M-scoring

Using the ACR CEUS LI-RADS diagnostic flowchart, there were 38, 1, 6, and 60 HCC nodules categorised as LR-M, LR-3, LR-4, and LR-5, respectively. One hundred, 0, 1, and 4 ICC nodules were categorised as LR-M, LR-3, LR-4, and LR-5, respectively.

If we used the M-score (cutoff value = -0.837) instead of LR-M and the modified LI-RADS algorithm, there were 12, 1, 7, and 85 HCC nodules categorised as M-score, LR-3, LR-4,

and LR-5, respectively. Ninety-four, 0, 1, and 10 ICC nodules were categorised as M-score, LR-3, LR-4, and LR-5, respectively (Table 3).

Diagnostic performance of the ACR LI-RADS and modified LI-RADS

The sensitivity and specificity of the ACR LI-RADS for diagnosing HCC were 57.14% and 96.19%, respectively. The

Table 2 Diagnostic performance of the LR-M and M-score for diagnosing ICC

	LR-M	M-score
Sensitivity	95.24	89.52
Specificity	63.81	88.57
PPV	72.46	88.68
NPV	93.06	89.42
Accuracy	79.52 (73.43, 84.77)	89.05 (84.02, 92.93)

Numbers are percentages, with 95% confidence intervals in parentheses
 ICC intrahepatic cholangiocarcinoma, PPV positive predictive value, NPV negative predictive value

Table 3 Classification of HCC and ICC by ACR LI-RADS or modified LI-RADS

ACR LI-RADS	Pathology		Modified LI-RADS	Pathology	
	HCC	ICC		HCC	ICC
LR-M	38	100	M-score	12	94
LR-3	1	0	LR-3	1	0
LR-4	6	1	LR-4	7	1
LR-5	60	4	LR-5	85	10
Total	105	105	Total	105	105

Numbers are number of cases

ACR American College of Radiology, LI-RADS Liver Imaging Reporting and Data System, ICC intrahepatic cholangiocarcinoma, HCC hepatocellular carcinoma

Table 4 Diagnostic performance of the ACR LI-RADS and modified LI-RADS for diagnosing HCC

	ACR LI-RADS	Modified LI-RADS
Sensitivity	57.14 (47.11, 66.76)	80.95 (72.13, 87.96)
Specificity	96.19 (90.53, 98.95)	90.48 (83.18, 95.34)
Disease prevalence at 50.0% ^b		
PPV	93.75 (84.76, 98.27)	89.47 (81.49, 94.84)
NPV	69.18 (61.01, 76.55)	82.61 (74.43, 89.04)
AUC ^a	0.767 (0.704, 0.822)	0.857 (0.802, 0.901)
Practical prevalence at 92.0% [21]		
Modified PPV	99.42 (95.64, 100.00)	98.99 (95.90, 99.92)
Modified NPV	16.33 (9.63, 25.16)	29.23 (17.45, 43.48)

Numbers are percentages, with 95% confidence intervals in parentheses ACR, American College of Radiology; *LI-RADS*, Liver Imaging Reporting and Data System; *HCC*, hepatocellular carcinoma; *AUC*, area under the curve; *PPV*, positive predictive value; *NPV*, negative predictive value

^a Numbers are raw data, with 95% confidence intervals in parentheses

^b Patients were included with propensity score matching at 1:1, the prevalence of which was at 50%

sensitivity and specificity of the modified LI-RADS for diagnosing HCC were 80.95% and 90.48%, respectively. The AUC of modified LI-RADS (AUC = 0.857) was much higher than ACR LI-RADS (AUC = 0.767, $p = 0.0001$).

Since we used the 1:1 propensity score matching for patient selection, the morbidity of HCC was 50% in this study. Consequently, the PPV and NPV of the ACR LI-RADS for diagnosing HCC were 93.75% and 69.18%, respectively. The PPV and NPV of the modified LI-RADS for diagnosing HCC were 89.47% and 82.61%, respectively. However, according to our previous study, the practical incidence rate of HCC in our institution was 92.0% [21]. Therefore, the modified PPV and NPV of the ACR LI-RADS for diagnosing HCC were 99.42% and 16.33%, respectively. The modified PPV and NPV of the modified LI-RADS for diagnosing HCC were 98.99% and 29.23%, respectively (Table 4).

Discussion

This study proposed a CEUS M-score as a substitute for LR-M, as well as a modified CEUS LI-RADS. Compared with the ACR CEUS LI-RADS, the modified CEUS LI-RADS had a higher sensitivity to diagnose HCC, and a higher specificity to diagnose ICC.

The differentiation between ICC and HCC in high-risk patients has been a challenging issue for the identification of HCC in focal liver lesions. The CEUS LI-RADS is designed to provide LR-5 100% specificity to HCC without biopsy. As indicated in our study, the diagnostic specificity of HCC achieved 96.19%. However, high specificity leads to low sensitivity and

false negative diagnosis of HCC. In LR-M nodules of our study, 27.5% HCC nodules were misclassified as non-HCC malignancy. We think that it was inaccurate to classify too many HCC nodules into LR-M because the category of LR-M is set to identify a malignant nodule, not necessarily HCC. Therefore, it is also necessary to improve the diagnostic sensitivity of HCC. Although the HCC specificity of modified LI-RADS was a little lower than ACR LI-RADS, the sensitivity has been greatly improved from 57.14 to 80.95%. The HCC diagnostic performance of modified LI-RADS was distinctly improved compared to the one of ACR LI-RADS. Upon using the practical prevalence of HCC in our institution, the PPV of modified LI-RADS remained quite high (98.99%).

One of the advantages of CEUS is real-time scanning. It can capture transient vascular architecture in the enhancement process along with the enhancement time and dynamic changes. We found that the vascular architecture of the two tumours is different. The unique vasculature development of HCC was the basket pattern or peripheral circular artery around the tumour [3]. Although the sensitivity of this feature was only 27.6%, the specificity for the identification of HCC was quite high (97.1%). Therefore, it could be added as an important ancillary feature in CEUS LI-RADS.

Although the LR-M in the CEUS LI-RADS represents various non-HCC malignancy, the most common malignancy aside from HCC in patients at risk for HCC is ICC [22]. A retrospective study showed that 40% (6/15) of LR-M lesions were HCCs, 13% (2/15) were hepatocholangiocarcinomas, and 47% (7/15) were cholangiocarcinomas [12]. Therefore, besides HCC, most LR-M nodules refer to ICC. LR-M is not a specific criterion to diagnose ICC, but it is mainly designed to include all ICC so that no ICC will be misdiagnosed as HCC. As shown in our study, the sensitivity of LR-M was 95.2% when LR-M was used as the diagnostic criterion for ICC, but the specificity was low (63.8%). As opposed to the study by Terzi E et al [11] which had no ICC misclassified as LR-5, ICCs were assigned as LR-5 in our study. Differentiating between ICC and HCC remains challenging. Therefore, a criterion to preserve high specificity for diagnosing ICC is necessary, and we need a more detailed definition of ICC to resolve this dilemma.

In this study, we investigated more specific CEUS features for ICC. In addition to rim enhancement, rapid washout, and marked washout proposed by ACR LI-RADS, we found that poorly circumscribed, intratumoural vein, and unclear boundary of the intratumoural non-enhanced area were also useful to diagnose ICC. Intratumoural vein was a unique CEUS feature that we have reported in previous study [18]. The unclear boundary of the intratumoural non-enhanced area may be consistent with its pathological findings, and is abundant in fibrous connective tissues with sparse tumour cells and blood vessels in the centre of the tumour [23]. Based on these features, we constructed an individualised M-score for predicting ICC. Compared with the LR-M, the M-score had a lower

sensitivity, but a much higher specificity from 63.8 to 88.6%, and a higher accuracy from 79.5 to 89.1%.

Our study has several limitations. First, we did not enrol benign lesions and other rare liver cancers to validate the diagnostic accuracy of the CEUS LI-RADS. Second, our study is a single centre study. A multicentre and prospective research is necessary to validate the applicability of CEUS LI-RADS in China. Finally, we did not compare the diagnostic performance of CEUS with that of MRI/CT. Although contrast enhanced MRI/CT are proposed as the diagnostic imaging standards by AASLD guidelines, their specificity or PPV for diagnosing HCC does not achieve 100% (95.2–97.3%) [24, 25]. Therefore, the optimal diagnostic algorithm or combination of MRI, CT, and CEUS is worth exploring in depth instead of simply deleting CEUS.

In conclusion, we developed a CEUS M-score for predicting ICC in high-risk patients. The modified LI-RADS and M-score had higher sensitivity for diagnosing HCC and higher specificity for diagnosing ICC than ACR LI-RADS. It was complementary with ACR LI-RADS. The HCC diagnostic performance of modified LI-RADS was improved in comparison to ACR LI-RADS.

Funding This study has received funding by the National Nature Science Foundation of China (No: 81701719), the Guangdong Science and Technology Foundation (No: 2016A020215042), and the Guangdong Medical Scientific Research Foundation (No: 201611610484333).

Compliance with ethical standards

Guarantor The scientific guarantor of this publication is Wei Wang.

Conflict of interest The authors of this manuscript declare no relationships with any companies whose products or services may be related to the subject matter of the article.

Statistics and biometry One of the authors has significant statistical expertise.

Informed consent Written informed consent was obtained from all subjects (patients) in this study.

Ethical approval Institutional Review Board approval was obtained.

Methodology

- retrospective
- diagnostic or prognostic study
- performed at one institution

References

1. Wildner D, Bernatik T, Greis C, Seitz K, Neurath MF, Strobel D (2015) CEUS in hepatocellular carcinoma and intrahepatic cholangiocellular carcinoma in 320 patients - early or late washout matters: a subanalysis of the DEGUM multicenter trial. *Ultraschall Med* 36:132–139
2. Bohle W, Clemens PU, Heubach T, Zoller WG (2012) Contrast-enhanced ultrasound (CEUS) for differentiating between hepatocellular and cholangiocellular carcinoma. *Ultraschall Med* 33:E191–E195
3. Dietrich CF, Cui XW, Boozari B, Hocke M, Ignee A (2012) Contrast-enhanced ultrasound (CEUS) in the diagnostic algorithm of hepatocellular and cholangiocellular carcinoma, comments on the AASLD guidelines. *Ultraschall Med* 33 Suppl(1):S57–S66
4. Bruix J, Sherman M, Practice Guidelines Committee, American Association for the Study of Liver Diseases (2005) Management of hepatocellular carcinoma. *Hepatology* 42:1208–1236
5. Bruix J, Sherman M, American Association for the Study of Liver Diseases (2011) Management of hepatocellular carcinoma: an update. *Hepatology* 53:1020–1022
6. Vilana R, Forner A, Bianchi L et al (2010) Intrahepatic peripheral cholangiocarcinoma in cirrhosis patients may display a vascular pattern similar to hepatocellular carcinoma on contrast-enhanced ultrasound. *Hepatology* 51:2020–2029
7. Omata M, Lesmana LA, Tateishi R et al (2010) Asian Pacific Association for the Study of the Liver consensus recommendations on hepatocellular carcinoma. *Hepatol Int* 4:439–474
8. Barreiros AP, Piscaglia F, Dietrich CF (2012) Contrast enhanced ultrasound for the diagnosis of hepatocellular carcinoma (HCC): comments on AASLD guidelines. *J Hepatol* 57:930–932
9. Quaiia E, Lorusso A, Grisi G, Stacul F, Cova MA (2012) The role of CEUS in the characterization of hepatocellular nodules detected during the US surveillance program—current practices in Europe. *Ultraschall Med* 33(Suppl 1):S48–S56
10. CEUS LI-RADS® v2017. Available via <https://www.acr.org/Clinical-Resources/Reporting-and-Data-Systems/LI-RADS/CEUS-LI-RADS-v2017>
11. Terzi E, Iavarone M, Pompili M et al (2018) Contrast ultrasound LI-RADS LR-5 identifies hepatocellular carcinoma in cirrhosis in a multicenter retrospective study of 1,006 nodules. *J Hepatol* 68:485–492
12. Wilson SR, Lyschik A, Piscaglia F et al (2018) CEUS LI-RADS: algorithm, implementation, and key differences from CT/MRI. *Abdom Radiol (NY)* 43:127–142
13. Stroppolini T, Gaeta GB, Mele A (2007) AASLD practice guidelines on chronic hepatitis B and HBV infection in Italy. *Hepatology* 46:608–609 author reply 609
14. Baek S, Park SH, Won E, Park YR, Kim HJ (2015) Propensity score matching: a conceptual review for radiology researchers. *Korean J Radiol* 16:286–296
15. Piscaglia F, Wilson SR, Lyschik A et al (2017) American College of Radiology Contrast Enhanced Ultrasound Liver Imaging Reporting and Data System (CEUS LI-RADS) for the diagnosis of hepatocellular carcinoma: a pictorial essay. *Ultraschall Med* 38:320–324
16. Catalano O, Nunziata A, Lobianco R, Siani A (2005) Real-time harmonic contrast material-specific US of focal liver lesions. *Radiographics* 25:333–349
17. Xu HX, Lu MD, Liu GJ et al (2006) Imaging of peripheral cholangiocarcinoma with low-mechanical index contrast-enhanced sonography and SonoVue: initial experience. *J Ultrasound Med* 25:23–33
18. Chen LD, Xu HX, Xie XY et al (2010) Intrahepatic cholangiocarcinoma and hepatocellular carcinoma: differential diagnosis with contrast-enhanced ultrasound. *Eur Radiol* 20:743–753
19. Zhang JX, Song W, Chen ZH et al (2013) Prognostic and predictive value of a microRNA signature in stage II colon cancer: a microRNA expression analysis. *Lancet Oncol* 14:1295–1306
20. Kono Y, Lyschik A, Cosgrove D et al (2017) Contrast enhanced ultrasound (CEUS) liver imaging reporting and data system (LI-RADS(R)): the official version by the American College of Radiology (ACR). *Ultraschall Med* 38:85–86

21. Huang XW, Liao B, Huang Y et al (2018) Non-invasive diagnostic criteria for hepatocellular carcinoma in hepatitis B virus-endemic areas: is cirrhosis indispensable? *Dig Dis* 36:228–235
22. Joo I, Lee JM, Lee SM, Lee JS, Park JY, Han JK (2016) Diagnostic accuracy of liver imaging reporting and data system (LI-RADS) v2014 for intrahepatic mass-forming cholangiocarcinomas in patients with chronic liver disease on gadoxetic acid-enhanced MRI. *J Magn Reson Imaging* 44:1330–1338
23. Xu HX, Chen LD, Liu LN, Zhang YF, Guo LH, Liu C (2012) Contrast-enhanced ultrasound of intrahepatic cholangiocarcinoma: correlation with pathological examination. *Br J Radiol* 85:1029–1037
24. Choi SH, Byun JH, Kim SY et al (2016) Liver imaging reporting and data system v2014 with gadoxetate disodium-enhanced magnetic resonance imaging: validation of LI-RADS category 4 and 5 criteria. *Invest Radiol* 51:483–490
25. Kim YY, An C, Kim S, Kim MJ (2018) Diagnostic accuracy of prospective application of the liver imaging reporting and data system (LI-RADS) in gadoxetate-enhanced MRI. *Eur Radiol* 28:2038–2046